

Enhanced solid element for modelling of reinforced concrete structures with bond-slip

Norberto Domínguez*¹, Marco Aurelio Fernández¹ and Adnan Ibrahimbegovic²

¹Sección de Estudios de Posgrado e Investigación (SEPI), ESIA-UZ, Instituto Politécnico Nacional.
Av. Juan de Dios Bátiz s/n edif. 12, 07738 México D.F., México

²Laboratoire de Mécanique et Technologie (LMT), ENS-Cachan/UPMC/CNRS/PRES
Univer Sud Paris 61 Avenue du Président Wilson, F-94230 Cachan, France

(Received May 14, 2009, Accepted January 26, 2010)

Abstract. Since its invention in the 19th century, Reinforced Concrete (RC) has been widely used in the construction of a lot of different structures, as buildings, bridges, nuclear central plants, or even ships. The details of the mechanical response for this kind of structures depends directly upon the material behavior of each component: concrete and steel, as well as their interaction through the bond-slip, which makes a rigorous engineering analysis of RC structures quite complicated. Consequently, the practical calculation of RC structures is done by adopting a lot of simplifications and hypotheses validated in the elastic range. Nevertheless, as soon as any RC structural element is working in the inelastic range, it is possible to obtain the numerical prediction of its realistic behavior only through the use of non linear analysis. The aim of this work is to develop a new kind of Finite Element: the “*Enhanced Solid Element (ESE)*” which takes into account the complex composition of reinforced concrete, being able to handle each dissipative material behavior and their different deformations, and on the other hand, conserving a simplified shape for engineering applications. Based on the recent XFEM developments, we introduce the concept of nodal enrichment to represent kinematics of steel rebars as well as bonding. This enrichment allows to reproduce the strain incompatibility between concrete and steel that occurs because of the bond degradation and slip. This formulation was tested with a couple of simple examples and compared to the results obtained from other standard formulations.

Keywords: enhanced solid element; reinforced concrete; x-fem, bond-slip.

1. Introduction

Reinforced concrete (RC) is used as the main material of construction in a great quantity of typical structures (buildings, bridges, foundations, houses, etc.) as well as for non conventional industrial structures, including nuclear central plants or maritime structures. Concrete is very useful not only for its mechanical properties but also for its thermal properties - that was the reason why concrete was initially employed for fire protection of steel frames. However, in spite of these interesting properties, RC is integrated by different materials which are subjected to particular degradation/damage process. Because of this, it is very important to predict and evaluate all of the dissipative phenomenon associated to the different materials; that means for example, cracking in concrete, plasticity in steel rebars, or bonding deterioration.

* Corresponding author, Professor Norberto Domínguez, E-mail: ndominguez@ipn.mx

In those cases, experimental studies accompanied by numerical simulations are necessary in order to reproduce any non linear response of the structural system when this one is subjected to different scenarios of loading. In which concerns to numerical analysis based on Finite Element modelling, it is very difficult-almost impossible - to build a detailed mesh where concrete, rebars and bonding are described separately with their different non linear material behavior. In addition, numerical modelling becomes heavy and slow. For these reasons, Reinforced Concrete is typically modelled as an homogenized material where concrete and rebars are joined by a perfect bonding. Based on these simplifications, a lot of standard FEM programs offers some "RC" elements which are able to reproduce the elastic response of the set, which is very convenient for structural design, but for understanding or predicting any specific behavior beyond the elastic limit, they are unable to do it. Nevertheless, some lines of research have tried to confront these problems by modelling shells where bonding degradation is represented as a loss of stiffness (Lackner and Mang 2001), or well, by modelling the behavior of all the ingredients (cement, gravel, rebar, bonding) without taking account of their particular deformations (Tikhomirov 1999). In the case of fire protection, some researchers (Ibrahimbegovic *et al.* 2009) have proposed to take account of the effects of temperature into the bonding degradation process.

In this work, we present a new RC Finite Element that is able to reproduce not only each non linear behavior of the main components (concrete, steel rebar and bonding) but also their corresponding deformations. This capacity of analyzing concrete and steel displacements separately, allows to calculate the realistic incompatibility of deformations which is the cause of degradation of bonding. Other advantages are: a better distribution of stresses inside the concrete body; a realistic location of the steel rebar; better prediction of cracking due to the effects of bonding deterioration, etcetera.

2. Formulation of the enhanced solid element

2.1 Preliminary concepts

XFEM is a recent methodology developed by Belytschko and co-workers (e.g. Moes *et al.* 1999, Sukumar *et al.* 2001), which originally focuses in studying crack propagation using the Finite Element Method, but avoiding the typical problem of remeshing as soon as the crack propagates inside the domain. In this model, the discontinuous displacement field within a finite element is simulated by a special set of enriched shape functions which takes account for the effects of the discontinuity. Based on the Principle of Partition of Unity, XFEM enriches the nodal degrees of freedom of each element affected by the crack, and automatically generates necessary enrichment functions for the elements around the crack path/tip when this one propagates to other elements.

For our case, we adopt the same XFEM principle, enriching the nodal degrees of freedom of elements where the steel rebar is explicitly embedded. For this, we reuse another technique called "*level set method*", which allows to locate the position of any geometric figure placed on a mesh with a different element distribution (Sukumar *et al.* 2001). Interpolation functions corresponding to each material: concrete, steel rebar and bonding, will be calculated over each sub-domain, using their derivatives to build the stiffness matrix of each component, and being completely assembled for the whole element stiffness matrix.

For building our element, we need to adopt the following hypotheses:

- We consider that all the external forces are applied exclusively on the concrete boundary.

- All volumetric forces corresponding to bonding and steel rebar are negligible.
- In which concerns to material behavior models, we will adopt:
 - for concrete, the local damage model developed by (Mazars 1986);
 - for steel, the elasto-plastic model developed by (Ibrahimbegovic and Brancherie 2003); and
 - for bonding, a thermodynamics damage model developed by (Dominguez 2005).

2.2 Description of the ESE

To illustrate some advantages of the Enhanced Solid Element, we are going to analyze a typical problem of reinforced concrete using different methodologies. We have a concrete structure where a steel rebar is completely embedded in the middle of the body. One of the faces of the concrete body is restrained against any kind of displacement, while a traction force is applied entirely on the other face (see Fig. 1). We want to find the global response of the structure by numerical simulation using finite elements. Simplifying the 3D problem in a 2D problem, it is possible to discretize it with a classical FE mesh, modelling only two sub-domains: concrete body (using 2D quadrilateral elements) and steel rebar (using 2D quadrilateral elements or axial truss elements) (see Fig. 2). In this standard modelling, bonding is considered perfect and displacements for concrete and rebar are the same. Other possibility is to discretize bonding as well, using 2D quadrilateral elements, but meshing becomes very complicated.

A second possibility of modelling is to use width-zero interface elements between steel rebar and concrete body in order to reproduce the effects of bonding (see Fig. 3). This kind of element has been developed by (Dominguez 2005) as well as (Fischinger *et al.* 2004), who developed a non-linear element to simulate time-dependent cracking of reinforced concrete members under service loads. The first one of Dominguez has shown good results to predict the cracking pattern distribution for reinforced concrete ties (Dominguez 2005), but it is not very practical for structures of big size.

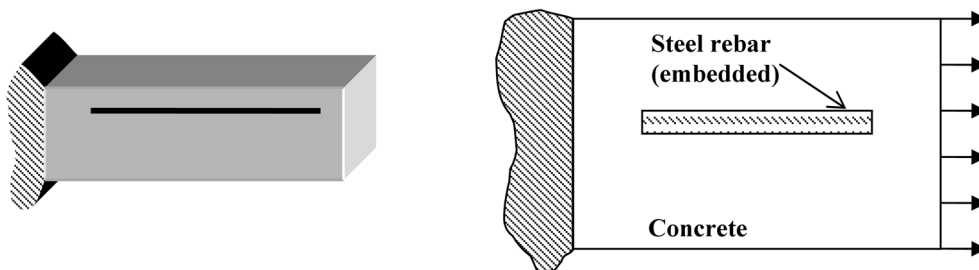


Fig. 1 3D RC structure analyzed as a 2D problem, subjected to traction forces

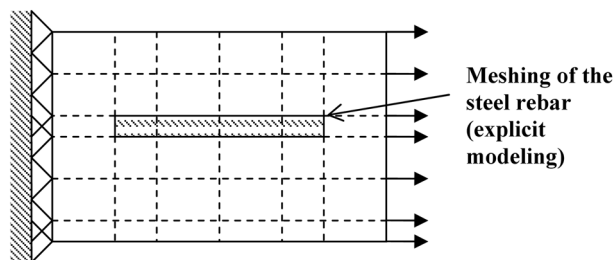


Fig. 2 Classical 2D modelling of the steel rebar mesh

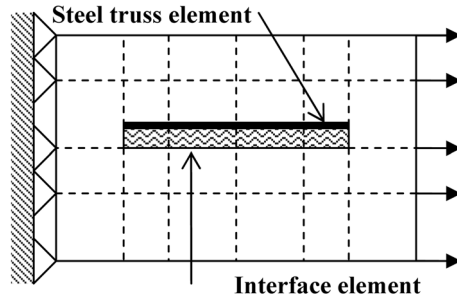


Fig. 3 Modelling of the steel rebar and bonding with interface elements

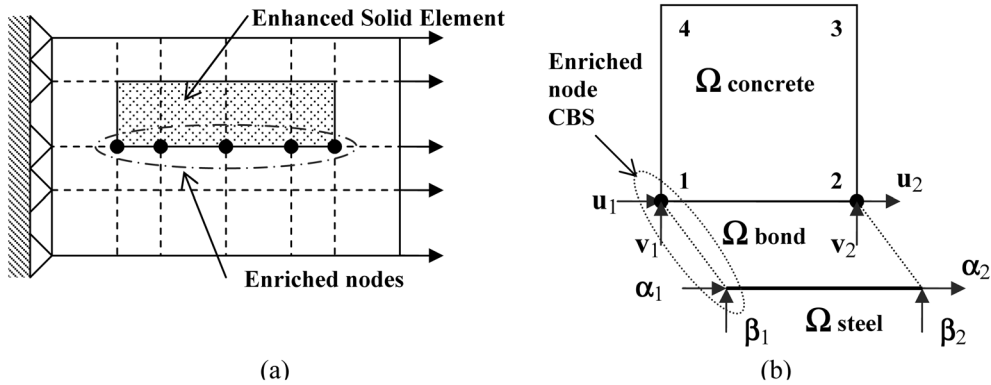


Fig. 4 “Enhanced Solid Element”: (a) modelling of the problem, (b) internal ESE components

For a user's point of view, the “*Enhanced Solid Element (ESE)*” consists in selecting a region of elements where the rebar is going to be placed, which is determined by the set of coordinates of the rebar edges. As well as it is done in XFEM, the *Level Set Method* construct a line between both points and verifies which elements are completely cut by this one, enriching all the nodes of the concerned elements with additional degrees of freedom (see Fig. 4(a)). In comparison to the other type of modelling, we reduce the complexity and the size of the mesh and, such that it is shown in Fig. 4(b), we can manage any sliding of the rebar respect to the concrete body.

From the same Fig. 4(b), we can appreciate the internal configuration of the Enhanced Solid Element: for a bidimensional formulation, it is a 4-node bilinear quadrilateral element with 2 nodes enriched with 2 additional degrees of freedom for node (12 total DOF for element). For numerical integration, we assign 4 points of Gauss for concrete, 1 or 2 points of Gauss for bonding, and 1 point of Gauss for the steel rebar (7 points of Gauss for one ESE). Mathematically, the ESE domain is defined as the assembling of three sub-domains as follows

$$\Omega^e = \Omega_{concrete} + \Omega_{steel} + \Omega_{bond} \tag{1}$$

In the last expression, Ω^e corresponds to the Enhanced Solid Element domain, while $\Omega_{concrete}$, Ω_{steel} and Ω_{bond} correspond respectively to concrete, steel and bonding domain. For simplicity, we will recall each sub-domain for their corresponding first letter, that means, *concrete* by *c*, *steel* by *s* and *bonding* by *b*. In the same way, each enriched node will be identified as a *CBS node* (concrete-bond-steel node).

2.2.1 Absolute and relative displacements in bonding

At this point, it is necessary to define two kind of displacements that are key-pieces for evaluate bonding behavior: absolute and relative displacements. In the typical resolution of a system of equations, the values of the displacement vector obtained as solution are expressed en absolute terms. However, the value of the sliding does not correspond exactly to this kind of displacement, because looking at its definition, sliding is the relative displacement between concrete and steel (see Fig. 5). In consequence, to evaluate the non linear behavior of bonding it is better to use this relative value.

From Fig. 5, we can deduce sliding as the difference between concrete and steel displacements, such that it is expressed in Eq. (2)

$$\alpha_i = u_i(x) + g_i(x) \tag{2}$$

In this expression, u_i is the nodal displacement associated to the continue part of the finite element solution, that means, the set of unknowns corresponding to the classical Degrees of Freedom (DOF); α_i is the nodal displacement associated to the discontinue part of the solution (in fact, the steel rebar); and g_i corresponds to the relative sliding between steel rebar and concrete body, which controls bonding degradation.

The transformation of displacements, from absolute to relative values and vice-versa, is possible thanks to the matrix of transformation T . This transformation can be expressed as follows

$$\begin{Bmatrix} u_i \\ \alpha_i \end{Bmatrix}_{i=1,2} = [T] \begin{Bmatrix} u_i \\ g_i \end{Bmatrix} \tag{3}$$

For a 2D case, this expression can be developed as follows

$$\begin{Bmatrix} u_1 \\ v_1 \\ u_2 \\ v_2 \\ \alpha_1 \\ \beta_1 \\ \alpha_2 \\ \beta_2 \end{Bmatrix} = \begin{bmatrix} 1 & 0 & 0 & 0 & 0 & 0 & 0 & 0 \\ 0 & 1 & 0 & 0 & 0 & 0 & 0 & 0 \\ 0 & 0 & 1 & 0 & 0 & 0 & 0 & 0 \\ 0 & 0 & 0 & 1 & 0 & 0 & 0 & 0 \\ 1 & 0 & 0 & 0 & 1 & 0 & 0 & 0 \\ 0 & 1 & 0 & 0 & 0 & 1 & 0 & 0 \\ 0 & 0 & 1 & 0 & 0 & 0 & 1 & 0 \\ 0 & 0 & 0 & 1 & 0 & 0 & 0 & 1 \end{bmatrix} \begin{Bmatrix} u_1 \\ v_1 \\ u_2 \\ v_2 \\ g_1^t \\ g_1^n \\ g_2^t \\ g_2^n \end{Bmatrix} \tag{4}$$

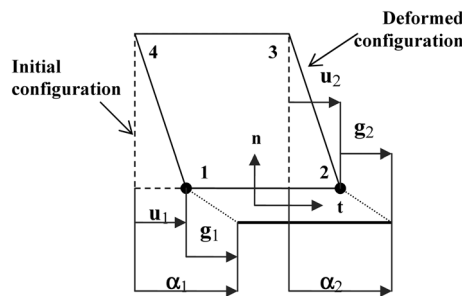


Fig. 5 Sliding description inside of the “Enhanced Solid Element”

In the last expression, g_1^n and g_2^n correspond to the relative displacements on the normal direction of the enriched nodes, while g_1^t and g_2^t correspond to the relative displacements on the tangential direction (sliding).

2.2.2 Nodal enrichment

For our particular case, the enriched approximation of the element nodal displacements may be written as follows

$$u^h(x) = \sum_{i=1}^4 N_i^c(x) u_i + \left[\sum_{i=1}^2 N_i^b(x) u_i + \sum_{i=1}^2 N_i^b(x) \alpha_i \right] + \sum_{i=1}^2 N_i^a(x) \alpha_i \quad (5)$$

Here, u_i is the vector of nodal displacements associated to the continue part of the solution, while α_i is the vector of enriched degrees of freedom for the CBS nodes, representing the absolute displacements of the steel rebar. N_i^c are the bilinear shape functions on the domain Ω_c associated to the 4-nodes of the element; N_i^b are the special shape functions written in the domain Ω_b associated to the CBS nodes of the element (on the edge, only 2 concerned nodes); and finally, N_i^a are the classical shape functions of a one-dimensional bar belonging to the rebar domain Ω_r .

From Eq. (5), it can be observed that bonding shape functions associate concrete displacements to the steel rebar displacements in absolute terms. In the same way, this equation can be rewritten for relative displacements as follows

$$u^h(x) = \sum_{i=1}^4 N_i^c(x)|_{\Omega_c} u_i + \sum_{i=1}^2 N_i^b(x)|_{\Omega_b} g_i + \sum_{i=1}^2 N_i^a(x)|_{\Omega_r} g_i \quad (6)$$

Here, g_i is the vector of enriched degrees of freedom for the CBS nodes, representing the relative displacement between the steel rebar and the concrete body (sliding).

2.2.3 The enriched shape functions

As well as it is done in the XFEM method, the enriched shape functions are classical shape functions affected by a particular function of discontinuity (it might be Heaviside, distance function, sign function, etc.). The construction of these shape functions is done over each sub-domain, and in consequence they are independent. From Fig. 6, we can identify the three sub-domains that constitutes the Enhanced Solid Element. For concrete and bonding sub-domains, the bilinear shape functions are similar to those of a classical 4-nodes quadrilateral element

$$N_a(\xi, \eta) = (1 + \xi_a \xi)(1 + \eta_a \eta) \quad (7)$$

In this expression, $a = 1, \dots, 4$ corresponds to the node number; ξ and η are the natural coordinates; and ξ_a, η_a are the coordinates of node a in the space of ξ .

At this point, we must pay attention to the nodes concerned by the bonding sub-domain: Even if nodes 3 and 4 belonging to the bonding region are placed on the same geometrical location as the nodes 1 and 2 of the concrete region, they are different, and they will be identified as nodes 1' and 2' (see Fig. 6). As well as it was done for a width-zero interface element (Domínguez 2005), we will introduce a parameter called h_{pen} , which allows to build the shape functions and the derivatives for the bonding region.

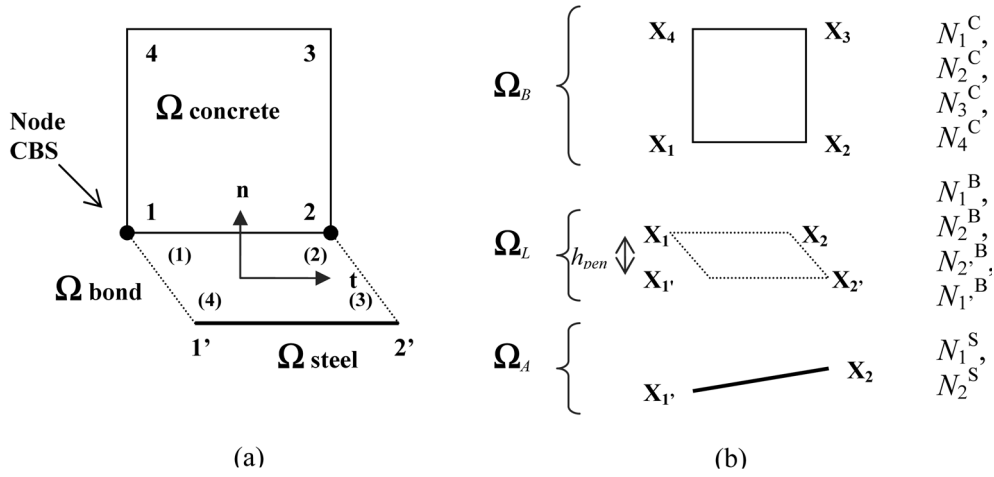


Fig. 6 Construction of the Shape Functions for the “enhanced Solid Element”: (a) pseudo-nodes for bonding, (b) each subdomain's geometric coordinates

2.3 Variational formulation

2.3.1 Strong formulation

We consider an open domain called Ω , formed by three subdomains: concrete (c), steel (s) and bonding (b); that means $\Omega^e = \Omega_c \cup \Omega_s \cup \Omega_b$. Its boundary is defined by Γ , which in the same way is constituted by the Dirichlet boundary conditions Γ_u (set of imposed displacements) and the Neumann boundary conditions Γ_t (set of external forces). That means

$$\Gamma = \Gamma_u \cup \Gamma_t \quad \text{and} \quad \Gamma_u \cap \Gamma_t = 0 \tag{8}$$

It is very important to remark that here $\Gamma = \Gamma_c$, because the other two subdomains, steel and bonding, are embedded into the concrete domain; it means that the whole set of external forces and imposed displacements are only being applied over the concrete boundary.

So, the strong form of the problem can be expressed as follows

- the equilibrium equation:

$$\nabla_m \cdot \sigma + b = 0 \quad \text{in} \quad \Omega \tag{9}$$

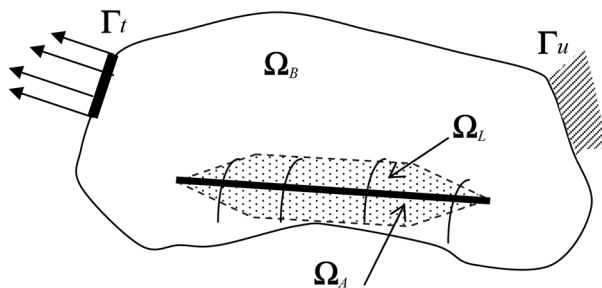


Fig. 7 Domain Ω containing the steel rebar Ω_s and bonding Ω_b

- the constitutive material law:

$$\sigma_m = c_m^{inelastic} \varepsilon_m \quad (10)$$

- the kinematics equation:

$$\varepsilon_m = \varepsilon_m(u, g) = \nabla_m^S(u, g) \quad (11)$$

- the Dirichlet boundary conditions:

$$u(x) = \bar{u} \quad \forall x \in \Gamma_u \quad (12)$$

- the Neumann boundary conditions:

$$\sigma \cdot n = \bar{t} \quad \forall x \in \Gamma_t \quad (13)$$

- traction continuity condition between materials:

$$\|\sigma \cdot n - \bar{t}\| = 0 \quad (14)$$

In the last expressions, n is the unit outward normal vector, σ_m corresponds to the Cauchy stress tensor for each material, and b is the body force (only for the concrete); ∇_m^S represents the symmetric part of the gradient operator, and $C_m^{inelastic}$ corresponds to the elastic-“inelastic” behavior tensor for each material.

2.3.2 Weak formulation

The weak form of the problem may be written as follows:

Being $u \in V$ a “test” displacement, candidate for the solution, and $a \in V_0$ “virtual” displacement, find (u) such that $\forall v \in V_0$

$$\int_{\Omega} \sigma(u) : \varepsilon(v) d\Omega = \int_{\Gamma_t} \bar{t} \cdot v d\Gamma_t + \int_{\Omega} b \cdot v d\Omega \quad (15)$$

It must be remarked that V_0 is the set of the displacement’s field that vanish on the essential boundary $\Gamma_u: V_0 = \{ v: \Omega \rightarrow \mathcal{R}^3 | v(x) = 0, \forall x \in \Gamma_u \}$.

2.4 Formulation of discrete equations

2.4.1 Discrete system for finite elements

Reformulating the Eq. (15) for a discrete problem, we will have

Find $u^h \in V^h \subset V$ such that $\forall v^h \in V_0^h$

$$\int_{\Omega} \sigma(u^h) : \varepsilon(v^h) d\Omega = \int_{\Gamma_t} \bar{t} \cdot v^h d\Gamma_t + \int_{\Omega} b \cdot v^h d\Omega \quad (16)$$

Here u^h and v^h are approximations of “test” and “virtual” displacement fields. By the way, if we consider the absolute displacements such that $u^h = \{u^h, \alpha^h\}$ and $v^h = \{\tilde{u}^h, \tilde{\alpha}^h\}$, so it is possible to rewrite the problem in the next terms

Find (u^h, α^h) , such that

$$\int_{\Omega} \sigma(u^h, \alpha^h) : \varepsilon(\tilde{u}^h, \tilde{\alpha}^h) d\Omega = \int_{\Gamma_t} \bar{t} \cdot \tilde{u}^h d\Gamma_t + \int_{\Omega} b \cdot \tilde{u}^h d\Omega \quad (17)$$

From this expression, if we consider that

$$f^{int}(u^{(i+1)}, \alpha^{(i+1)}) = \int_{\Omega} \sigma(u^h, \alpha^h) : \varepsilon(\tilde{u}^h, \tilde{\alpha}^h) d\Omega \tag{18}$$

$$f^{ext} = \int_{\Gamma_i} \tilde{t} \cdot \tilde{u}^h d\Gamma_i + \int_{\Omega} b \cdot \tilde{u}^h d\Omega \tag{19}$$

It is possible to reduce the weak formulation to

$$\begin{aligned} & \text{Given} && u^{(i)}, \alpha^{(i)} \\ & \text{find} && u^{(i+1)}, \alpha^{(i+1)} \\ & \text{such that} && f^{int}(u^{(i+1)}, \alpha^{(i+1)}) = f^{ext} \end{aligned} \tag{20}$$

Linearizing the last expression (20) drives to the next system

$$\mathbb{A}_{e=1}^{N_{elem}} \left[K^e \cdot \begin{Bmatrix} u_i \\ g_i \end{Bmatrix} = f^{ext} - r^{e(i)} \right] \tag{21}$$

Here, $\mathbb{A}_{e=1}^{N_{elem}}$ is the assembly operator applied to the N_{elem} of the discretization; K^e is the element stiffness matrix; $\{u_i, \alpha_i\}$ corresponds to the vector of nodal unknowns; f^{ext} is the external force vector and $r^{e(i)}$ is the residual.

2.5 Numerical implementation of the enhanced solid element

2.5.1 Numerical integration

For numerical integration, we will implement three groups of points of Gauss distributed in the different sub-domains, according to Fig. 8.

For our particular case, we will rewrite Eq. (22) as follows

$$\mathbb{A}_{e=1}^{N_{elem}} [f_c^{int}(u)^{(i)} + f_b^{int}(u, \alpha)^{(i)} + f_s^{int}(\alpha)^{(i)} = f^{ext} - r^{e(i)}] \tag{22}$$

Even more, reintegrating over all the integration points, it could be possible to rewrite

$$\mathbb{A}_{e=1}^{N_{elem}} \left[K_C|_{PG=1-4} \cdot (u)^{(i)} + K_b|_{PG=5-6} \cdot \begin{Bmatrix} u^{(i)} \\ \alpha^{(i)} \end{Bmatrix} + K_s|_{PG=7} \cdot (\alpha)^{(i)} = f^{ext} - r^{e(i)} \right] \tag{23}$$

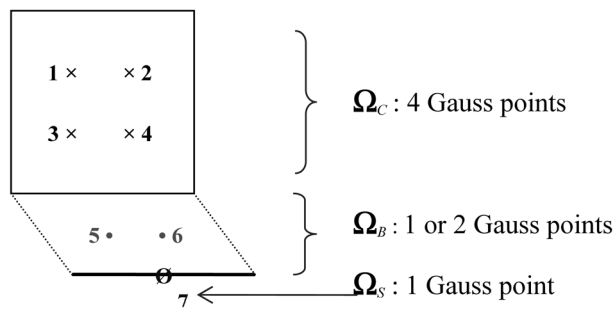


Fig. 8 Numerical integration of the Enhanced Solid Element with 6 or 7 integration points

Analyzing each domain, the internal forces on each node “ j ” belonging to ESE will be calculated as follows

$$f_c^{int} = K_c|_{PG=1-4} \cdot (\Delta u)^{(i)} = \left[\begin{array}{cc} k_{(uu)}^c & k_{(uv)}^c \\ k_{(vu)}^c & k_{(vv)}^c \end{array} \right] \cdot \left\{ \begin{array}{c} \Delta u_j^{(i)} \\ \Delta v_j^{(i)} \end{array} \right\} \Bigg|_{j=1-4} \quad (24)$$

$$f_b^{int} = K_b|_{PG=5-6} \cdot \left\{ \begin{array}{c} \Delta u^{(i)} \\ \Delta \alpha^{(i)} \end{array} \right\} = \left[\begin{array}{cccc} k_{(uu)}^b & k_{(uv)}^b & k_{(u\alpha)}^b & k_{(u\beta)}^b \\ k_{(vu)}^b & k_{(vv)}^b & k_{(v\alpha)}^b & k_{(v\beta)}^b \\ k_{(\alpha u)}^b & k_{(\alpha v)}^b & k_{(\alpha\alpha)}^s & k_{(\alpha\beta)}^s \\ k_{(\beta u)}^b & k_{(\beta v)}^b & k_{(\beta\alpha)}^s & k_{(\beta\beta)}^s \end{array} \right] \cdot \left\{ \begin{array}{c} \Delta u_j^{(i)} \\ \Delta v_j^{(i)} \\ \Delta \alpha_j^{(i)} \\ \Delta \beta_j^{(i)} \end{array} \right\} \Bigg|_{j=1-2} \quad (25)$$

$$f_s^{int} = K_s|_{PG=7} \cdot (\Delta \alpha)^{(i)} = \left[\begin{array}{cc} k_{(\alpha\alpha)}^s & k_{(\alpha\beta)}^s \\ k_{(\beta\alpha)}^s & k_{(\beta\beta)}^s \end{array} \right] \cdot \left\{ \begin{array}{c} \Delta \alpha_j^{(i)} \\ \Delta \beta_j^{(i)} \end{array} \right\} \Bigg|_{j=1} \quad (26)$$

Last expressions for bonding and steel apply exclusively to the enriched CBS nodes of ESE. The sub-matrix and vectors which constitute the discrete

$$k_{ij}^c = \int_{\Omega^c} (B_i^c)^T C_c^{inel} B_j^c d\Omega_c \quad (i, j = u, v) \quad (27)$$

$$k_{ij}^b = \int_{\Omega^b} (B_i^b)^T C_b^{inel} B_j^b d\Omega_b \quad (i, j = u, v, \alpha, \beta) \quad (28)$$

$$k_{ij}^s = \int_{\Omega^s} (B_i^s)^T C_s^{inel} B_j^s d\Omega_b \quad (i, j = \alpha, \beta) \quad (29)$$

And for the external forces, we take account only for those applied into the concrete boundary

$$f^{ext} = \int_{\Gamma_i} N_i^c \cdot \bar{t} d\Gamma_i + \int_{\Omega} N_i^c \cdot b^b d\Omega \quad (30)$$

Using the matrix of transformation $[T]$ (see 3) we will have

$$\tilde{K}_m = (T)^T \cdot K_m \cdot T; \quad (m = c, b, s) \quad (31)$$

Here, \tilde{K}_m corresponds to the stiffness matrix for each single material, obtained in relative displacements.

2.5.2 Calculation of strains and stresses

The constitutive relationships between strains and stresses for each material are written in their respective sub-domain. So, for the Points of Gauss assigned to concrete (1 to 4) we will have the next expressions

$$\varepsilon_c^h(x)|_{PG=1-4} = \sum_{a=1}^4 B_a^c \cdot u^h(x) \quad (32)$$

$$\sigma_c^h(x)|_{PG=1-4} = C_c^{inel} \cdot \varepsilon_c^h(x) \quad (33)$$

For bonding, we will have (with 1 or 2 points of Gauss)

$$\varepsilon_b^h(x)|_{PG=5-6} = \sum_{a=1}^2 B_a^b \cdot u^h(x) + \sum_{a=1}^2 B_a^b \cdot \alpha^h(x) \quad (34)$$

$$\sigma_b^h(x)|_{PG=5-6} = C_b^{inel} \cdot \varepsilon_b^h(x) \quad (35)$$

Finally, for the steel rebar we will have

$$\varepsilon_s^h(x)|_{PG=7} = \sum_{a=1}^2 B_a^s \cdot \alpha^h(x) \quad (36)$$

$$\sigma_s^h(x)|_{PG=7} = C_s^{inel} \cdot \varepsilon_s^h(x) \quad (37)$$

2.5.3 Shape function derivatives

In a similar way, three groups of shape functions corresponding to each sub-domain have been implemented for the *Enhanced Solid Element*. Their derivatives will be used to construct the respective elementary stiffness matrix, as it is shown in the next lines.

For the concrete domain Ω_c , the matrix of shape function derivatives for each node j is written as follows

$$[B_i^c]_j = \begin{bmatrix} N_{i,x}^c & 0 \\ 0 & N_{i,y}^c \\ N_{i,y}^c & N_{i,x}^c \end{bmatrix} \quad (i = u, v); \quad (j = 1, \dots, 4) \quad (38)$$

The “*jacobian*” of this sub-domain is calculated from the geometrical coordinates of the 4-nodes of the ESE. For bonding domain, the matrix B is written as

$$[B_i^b]_j = \begin{bmatrix} N_{i,x}^b & 0 \\ 0 & N_{i,y}^b \\ N_{i,y}^b & N_{i,x}^b \end{bmatrix} \quad (i = u, v, \alpha, \beta); \quad (j = 1, 2) \quad (39)$$

For construction of the last matrix, it is necessary to remark that geometric space of bonding should be zero, because the width of this region is zero (Hughes 2000). However, the parameter h_{pen} acts as a “pseudo”-width for this region, delimited by the nodes 1-2-2'-1'. Finally, for the steel rebar we reuse the classical derivatives for a 2D axial bar

$$[B^s] = \left[-\frac{1}{l_0} + \frac{1}{l_0} \right] \quad (40)$$

2.6 Numerical resolution procedure

In order to solve the equation system obtained from the precedent formulation, we are going to use a classical global resolution method: that means, all equilibrium equations will be solved

simultaneously, in order to find the best approximation for total strain $\varepsilon_{n+1}^{(i)}$ in each point of Gauss for the instant t_{n+1} at the i^{th} iteration. Locally, the problem is reduced to solve all of the internal variables that satisfies any stress admissibility. Globally, we will solve the complete system of equations from the assembling of all elementary stiffness matrix for the whole structure by using the *Newton-Raphson* method (see Ibrahimbegovic 2009).

The procedure is as follows:

1. Initially, reading of geometrical characteristics and material properties of the Enhanced Solid Element.
2. Reading of internal variables for each subdomain, in every point of Gauss, from the last stocked step of time. That means, for instant t_n we will have

$$\begin{aligned}\varepsilon_m|_n &= \varepsilon_m(x, t_n) & \text{for } (m=c, b, s) & \text{total strain} \\ \varepsilon_m^{inel}|_n &= \varepsilon_m^{inel}(x, t_n) & \text{for } (m=c, b, s) & \text{any inelastic strain} \\ \zeta_m^k|_n &= \zeta_m^k(x, t_n) & \text{for } (m=c, b, s) & \text{any internal variable "k"}\end{aligned}$$

3. predictive calculation of elastic stresses-strains

$$\begin{aligned}\text{Given } & \varepsilon_m|_n^{(i)}, \varepsilon_m^{inel}|_n^{(i)}, \zeta_m^k|_n^{(i)} & \text{over each sub-domain} \\ \text{find } & \sigma_m|_{n+1}, \varepsilon_m|_{n+1}, \varepsilon_m^{inel}|_{n+1}, \zeta_m^k|_{n+1}\end{aligned}$$

4. Evaluation of non linear behavior starting by comparing to the elastic limit of each material.
5. Non linear calculations of different material behaviors on each Gauss point
 - (a) *Damage in concrete*: explicit calculation of the damage scalar variable.
 - (b) *Bonding deterioration*: explicit-implicit calculation of the damage and crack friction variables.
 - (c) *steel rebar plasticity*: classical elasto-plastic calculation.
6. Deduction of the behavior matrix for each sub-domain

$$C_m^{inel}|_{n+1}^{(i)} = \frac{\dot{\sigma}_m}{\dot{\varepsilon}_m}$$

7. Construction of the stiffness matrix for each sub-domain

$$k_m^m|_{n+1}^{(i)} = \int_{\Omega} (B^m)^T \cdot C_m^{inel}|_{n+1}^{(i)} \cdot B^m d\Omega_m$$

8. Integration of the elementary stiffness matrix as well as the residual part for the Enhanced Solid Element

$$\begin{aligned}K^{ESE}|_{n+1}^{(i)} &= \sum_{m=c, b, s} k_m^m|_{n+1}^{(i)} \\ R^{ESE}|_{n+1}^{(i)} &= f^{ext}|_{n+1} - \sum_{m=c, b, s} f_m^{int}|_{n+1}^{(i)}\end{aligned}$$

9. Assembling of all elementary stiffness matrix in a global stiffness matrix

$$\sum_{e=1}^{N_{elem}} \{K_{n+1}^{e(i)} \cdot \Delta u_{n+1}^{(i)}\} = \sum_{e=1}^{N_{elem}} \{f_{n+1}^{e,ext} - f_{n+1}^{e,int(i)}\}$$

Finally, the global resolution of the system of equations is done by using a classical iterative method (*Newton-Raphson* method, in our case), without affecting the general architecture of the employed standard FEM code.

3. Numerical validation

In order to test the *Enhanced Solid Element*, we will simulate two different structures using diverse formulations, and comparing the results.

3.1 Simulation of a RC tie

A RC tie is a simple structure which is widely used for studying cracking in concrete provoked for the stress transference from the rebar to the concrete body, taking account of bonding deterioration. A lot of experimental studies has been done, and we can cite the works of (Clement 1987, Daoud 2003).

For numerical validation, we simulate a tie where concrete, steel and bonding have only elastic behaviors. Its dimensions are: 550 mm of length, 300 mm of height, one unit of depth; the steel rebar has a diameter of 8 mm (see Fig. 9). The traction forces as well as the restrained displacements are applied exclusively on the concrete boundary without any contact on steel rebar. In which concerns to materials, we have chosen for an ordinary concrete a Young modulus of 3.41×10^4 MPa and a Poisson coefficient of 0.2; for the steel rebar, a Young modulus of 2.1×10^5

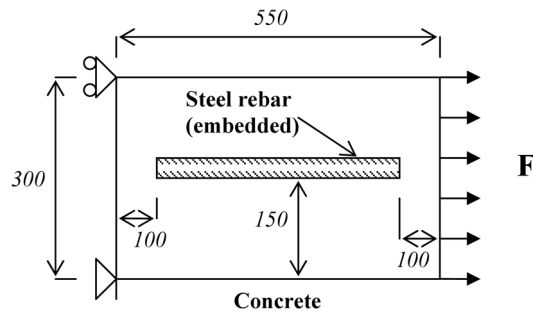


Fig. 9 Characteristics of RC tie for numerical validation

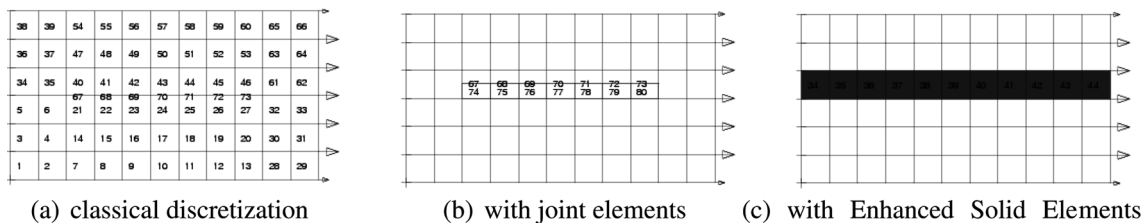


Fig. 10 Different discretizations for modelling the RC tie

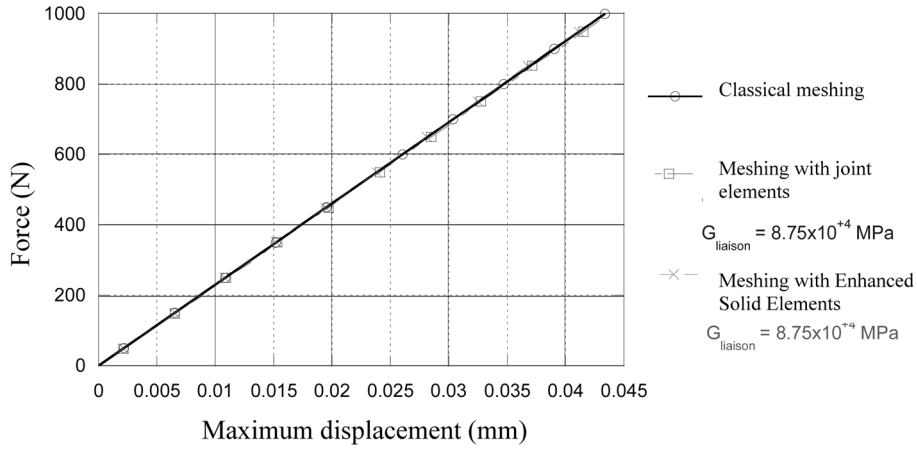


Fig. 11 Comparison of force vs. displacement relationship between different formulations

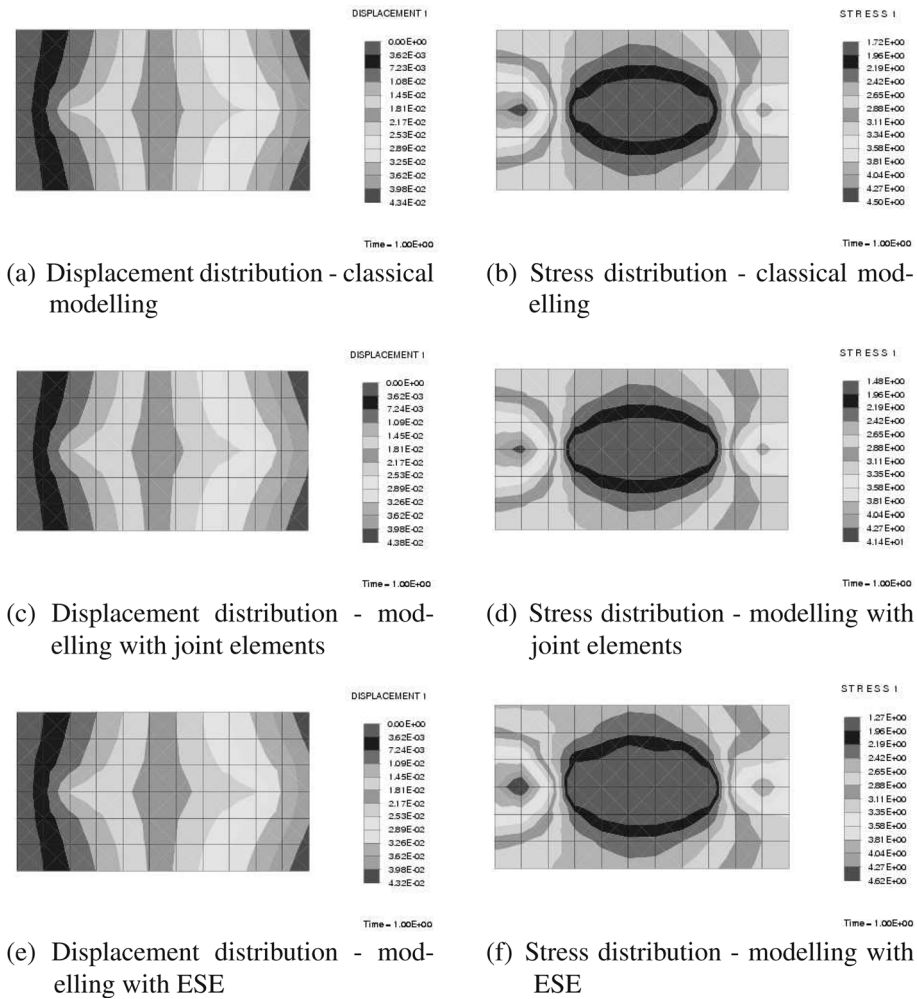


Fig. 12 Comparison of stresses and displacements configurations between different types of modelling

MPa and a Poisson coefficient of 0.3, with a transversal section of 50 mm². For bonding (used with joint elements and ESE), we assigned an elastic behavior with a Young modulus of 2.1×10⁵ MPa and a Poisson coefficient of 0.3; the parameter h_{pen} has been calculated as it is explained in (Dominguez 2005), having a value of 0.64 mm.

The first proposal of solution consists in a classical modelling based on plane strain analysis with standard 4-node quadrilateral elements for concrete (elements 1 to 66) and axial truss elements for steel rebar (elements 67 to 73). Rebar nodes are connected directly to the concrete nodes without any interface element (see Fig. 12(a)). In the second proposal we added non-width joint elements that links the concrete nodes to steel rebar nodes (corresponding to element numbers 74 to 80, in Fig. 12(b)). In the third proposal, we have identified the region where the rebar will be placed, and we have chosen a band of elements to be enriched. The rest of the elements will be modelled as standard 4-node quadrilateral elements. To locate geometrically the rebar respect to the mesh, it is only necessary to specify the coordinates of the rebar edges, and thanks to the implementation of the “level set method”, each element determines if it is or not concerned by the steel rebar. Looking at Fig. 12(c), we can appreciate that, even if the enriched region concerns to the band of elements 34 to 44, only elements 35 to 43 will be activated during calculations.

Applying an imposed traction force of 1 KN and comparing the results obtained from the three simulations, we can appreciate that all of them gives the same global relationship Force vs. Displacement (see Fig. 11). In the same way, we compared the stress and displacement distributions in the X direction, and it can be appreciated that three configurations are practically the same (see Fig. 12); even more, the concentration of stresses around the rebar edges are reproduced correctly in all cases.

3.2 Simulation of a three-point-bending beam

In order to test the capacity of the Enhanced Solid Element to reproduce any non linear behavior, we modelled a three-point-bending beam (see Fig. 13) based on the same three formulations used previously, but instead of adopting any elastic behavior for all materials, we implemented the following non linear models for materials:

- for concrete, we implemented the Mazars damage model, as it is explained in (Mazars 1986).
- for steel, a simple elastic model.
- for bonding, the thermodynamics damage model developed by (Dominguez 2005).

It is important to remark that these models and their parameters were employed identically in the three formulations.

So, for the first simulation based on a typical meshing, we use 366 nodes and 360 elements (300 4-

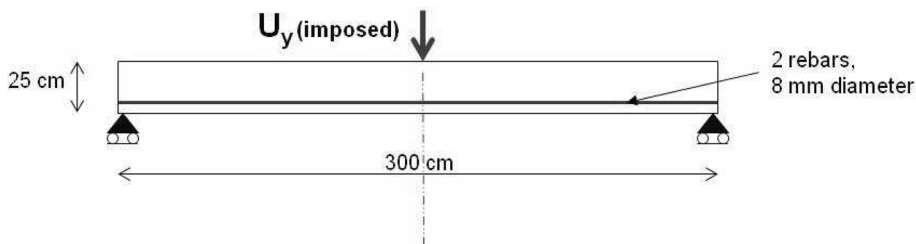


Fig. 13 Description of the three-point-bending beam

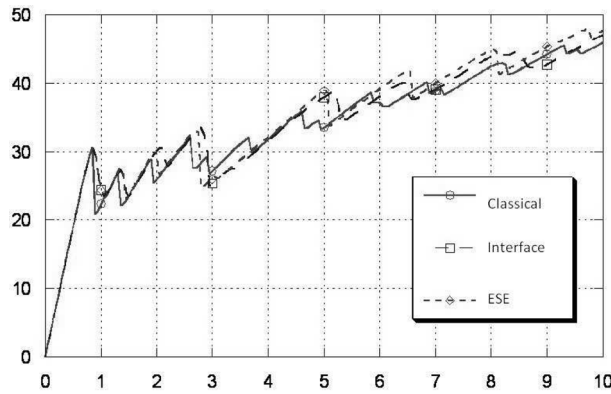


Fig. 14 Comparison of non linear force - displacement relationship between different formulations

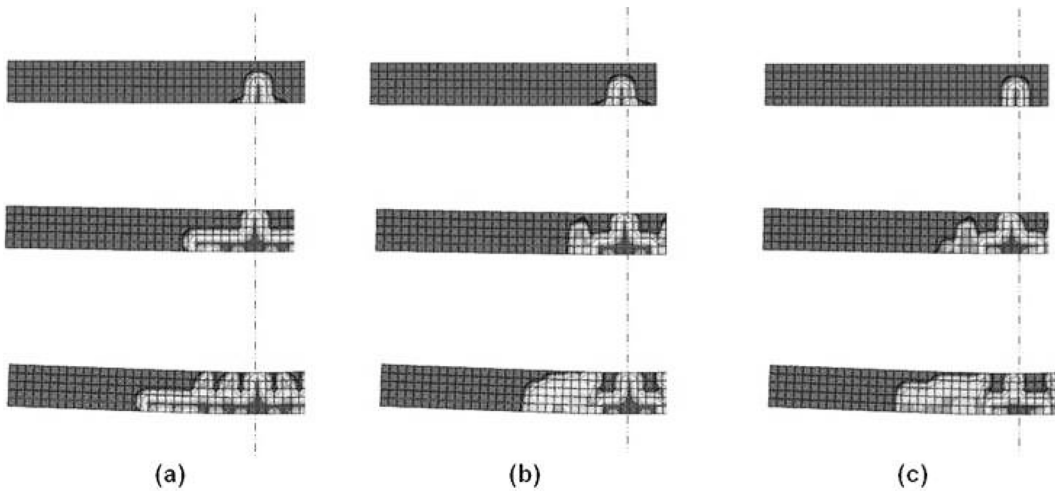


Fig. 15 Comparison of concrete damage between the three formulations: (a) classical modelling, (b) with interface element, (c) with ESE

node QUAD elements for concrete and 60 axial BAR elements for steel rebar); considering 2 DOF per node, we have $732 \text{ dof} - 2 \text{ restrained dof} = 730$ equations to solve with this formulation. For the second simulation, in which we used joint elements for bonding modelling, we have 427 nodes and 420 elements (300 4-node QUAD elements for concrete, 60 joint elements for bonding and 60 axial BAR elements for steel rebar); that means, $854 \text{ dof} - 2 \text{ restrained dof} = 852$ equations to solve with this formulation. Finally, for the third simulation using ESE, we have 366 nodes and 300 elements (240 4-node QUAD elements for simple concrete and 60 Enhanced Solid Elements for reinforced concrete); for this formulation, we have $854 \text{ dof} - 2 \text{ restrained dof} = 852$ equations to solve.

The numerical test consists in increasing the imposed displacement at the center of the beam, which is simply supported on both extremes. As soon as a crack appears, a falling of resistance is observed in Fig. 14. Commonly, cracking starts at beam's bottom and propagates to the top, making that steel rebar takes all of the tension stresses without any participation of concrete. A graphical comparison of results showing concrete damage are presented in Fig. 15. Thanks to the implementation of the same concrete damage model in the three formulations, it is possible to

reproduce concrete cracks in the beam, but the bonding effects change the crack pattern distribution, as it is shown in this same figure. Reviewing case (a) where bonding is considered perfect, as displacement increases, the damage of concrete is distributed along the steel rebar, instead of concentrating around a central macrocrack, as should be expected for the loss of bonding. The other two formulations (case (b) and (c)) represents much better this effect, since they improve the distribution of stress field around the steel rebar. In which concerns to numerical stability and robustness, the Enhanced Solid Element formulation shows a good behavior and the structural response is practically the same as that obtained with a formulation based on joint elements.

4. Conclusions

In this work we have presented the formulation of a new finite element, specifically adapted for Reinforced Concrete structures, called the *Enhanced Solid Element*. This element formulation is inspired by XFEM techniques and basically consists in growing the number of degrees of freedom of the nodes concerned by the steel rebar and bond. This enrichment allows to define delimited regions for each one of the main ingredients of reinforced concrete: concrete mass, steel rebar, and bonding. The main characteristic of this element is not only its capacity to reproduce the non linear behavior of each concerned material, but also - and most important - to calculate their respective particular kinematics: supported by this, it is possible to evaluate the displacement incompatibility between concrete and rebar which is the cause of bonding deterioration.

In general, the results report that the use of Enhanced Solid Elements can be very interesting for modelling complex structures in comparison to the typical modelling of Reinforced Concrete structures where the three ingredients are homogenized without any real opportunity for studying the structural response in the non linear range. The calculations with the ESE formulation shows robustness and numerical stability, as well as a good convergence as soon as the non linear behavior of different materials is initiated. Finally, we must highlight the main potentiality of the *Enhanced Solid Element*: the ease of use for simulating rebars and bonding inside a complex concrete structure taking account of their non linear behavior.

References

- Clément, J.L. (1987), *Interface acier-béton et comportement des structures en béton armé: caractérisation - modélisation*, Thèse de l'Université Paris VI, France.
- Daoud, A. (2003), *Étude expérimentale de la liaison entre l'acier et le béton autoplaçant - contribution à la modélisation numérique de l'interface*, Thèse de l'INSA de Toulouse, France.
- Dominguez, N. (2005), *Étude de la liaison acier-béton: de la modélisation du phénomène à la formulation d'un élément fini enrichi "béton armé"*, Thèse de doctorat de l'École Normale Supérieure de Cachan, France.
- Dominguez, N., Brancherie, D., Davenne, L. and Ibrahimbegovic, A. (2005), "Prediction of crack pattern distribution in reinforced concrete by coupling a strong discontinuity model of concrete cracking and a bond-slip of reinforcement model", *Eng. Comput.*, **22**(5-6), 558-582.
- Fischinger, M., Isakovic, T. and Kante, P. (2004), "Modelling time-dependent cracking in reinforced concrete using bond-slip interface elements", *Comput. Concrete*, **1**(2), 55-73.
- Hughes, J.R.T. (2000), *The finite element method. Linear static an dynamic finite element analysis*, Dover Publications, Inc., Mineola, New York.
- Ibrahimbegovic, A. and Brancherie, D. (2003), "Combined hardening and softening constitutive model for plasticity:

- precursor to shear slip line failure”, *Computat. Mech.*, **31**, 88-100.
- Ibrahimbegovic, A. (2009), *Nonlinear solid mechanics: theoretical formulations and finite element solution methods*, Springer, Berlin.
- Ibrahimbegovic, A., Boulkertous, A., Davenne, L., Muhasilovic, M. and Pokrklic, A. (2010), “On modeling of fire resistance tests on concrete and reinforced-concrete structures”, *Comput. Concrete*, **7**(4).
- Lackner, R. and Mang, H.A. (2001), “Adaptive FE analysis of RC shells. II: applications”, *J. Eng. Mech. - ASCE*, **127**(12), 1213-1222.
- Mazars, J. (1986), “A description of micro- and macro-scale damage of concrete structures”, *J. Eng. Fracture Mech.*, **45**(5-6), 729-737.
- Moes, N., Dolbow, J. and Belytschko, T. (1999), “A finite element method for crack growth without remeshing”, *Int. J. Numer. Meth. Eng.*, **46**, 131-150.
- Sukumar, N., Moes, N., Moran, B. and Belytschko, T. (2001), “Modeling holes and inclusions by level sets in the extended finite-element method”, *Comput. Method. Appl. M.*, **48**, 1549-1570.
- Tikhomirov, D. and Stein, E. (1999), “Anisotropic damage-plastic modelling of reinforced concrete”, *European Conference on Computational Mechanics (ECCM'99)*, Munchen, Germany.